

# Temperature dependence of dark current in a CCD

Ralf Widenhorn, Morley M. Blouke,\* Alexander Weber, Armin Rest,\*\* Erik Bodegom‡  
Department of Physics, Portland State University, Portland, OR 97207

\*Scientific Imaging Technologies, Tigard, OR 97223,

\*\*Astronomy Department, University of Washington, Seattle, WA 98195

## ABSTRACT

We present data for dark current of a back-illuminated CCD over the temperature range of 222 to 313 K including dark current spikes that are notorious for the wide range of activation energies. As a first attempt to analyze the behavior, we used the Arrhenius law, and found that the analysis of the data leads to the relation between the prefactor and the apparent activation energy in accordance with the classical Meyer-Neldel rule. However, a more detailed analysis shows that the apparent activation energy varies with temperature in the range investigated. This transition can be explained by the larger relative importance at high temperatures of the diffusion dark current and at low temperatures by the depletion dark current. Dark current spikes are pronounced at low temperatures and can be explained by concentrations of deep level impurities in those particular pixels. We show that fitting the data with the impurity concentration as the only variable can explain the dark current characteristics of all the pixels on the chip.

**Keywords:** depletion dark current, diffusion dark current, Meyer-Neldel rule

## 1. INTRODUCTION

The average dark current of a CCD is well described by the known thermal generation rates discussed below. As anyone who has investigated dark spikes knows, their behavior can be apparently quite pathological and seemingly defy the known rules. In an effort to better understand the dark current and the dark current spikes, we investigated the dark current for a backside-illuminated CCD housed in SpectraVideo camera (Model: SV512V1) manufactured by PixelVision, Inc.. The chip was a three phase, n-buried channel, three-level polysilicon, thinned device (12.3 mm x 12.3 mm, 512 x 512 pixels, manufactured by SiTe Inc.) with an individual pixel size of 24  $\mu\text{m}$  x 24  $\mu\text{m}$  operated in the Multi-Pinned Phase (MPP) mode. In order to minimize noise, the dark current associated with each pixel was determined as the average of several frames. 50 images were taken each for the following exposure times: 3, 5, 10, 20, 50, 100 s, 20 images each for 250 and 500 s and 10 images where taken for 1000 s. Dark frames for all exposure times were taken at 222, 232, 242, 252 and 262 K, for exposure times up to 500 s at 271 K, for exposure times up to 250 s at 281 K and for exposure times up to 50 s at 291 K. None of the of 472 x 472 pixel subframes showed pixels which were saturated and the dark current increased linearly with increasing exposure time. Hence, we could calculate the dark current by fitting the number of electrons collected versus the exposure time.[1]

## 2. THE MEYER-NELDEL RULE FOR DARK CURRENT IN A CCD

The Meyer-Neldel rule (MNR) is an empirical law first espoused by W. Meyer and H. Neldel in 1937, and is observed frequently for processes which follow the Arrhenius law.[2] The MNR is found in various fields and for several different processes, e.g. for diffusion [3,4], or the conductivity of semiconductors.[5-7] Although different explanations have been proposed, none is universally accepted, and the discussion as to what causes the MNR is not settled. It has been argued that the MNR arises due to an exponential density of state distribution that induces a shift in the Fermi level.[8] Others see the origin in the entropy of multiple excitations.[9,10]

For dark current, a process that follows the Arrhenius law,

$$De = De_0 \exp\left(-\frac{\Delta E}{kT}\right) \quad (1)$$

where  $De$  is the dark current in  $e/s$  and  $\Delta E$  is the activation energy. The MNR states that the logarithm of the exponential prefactor depends linearly on the activation energy. Hence, for the dark current:

$$De_0 = De_{00} \exp\left(\frac{\Delta E}{E_{MN}}\right) \quad (2)$$

where  $De_{00}$  and  $E_{MN}$  are positive constants.

According to Eq. (1) all data points in a plot of the logarithm of  $De$  versus the inverse temperature should lie on a straight line. The activation energy of the process is the absolute value of the slope of this line. Figure 1 shows the Arrhenius plot and linear fits to the data points of four random pixels. The upper three curves represent what would usually be referred to as dark current spikes. Note the different activation energies. Although a straight line fit does not model the data perfectly, the assumption of describing dark current with Eq. (1) seems reasonable. We fit all 222,784 individual pixels according to the Arrhenius law and obtained 222,784 pairs of exponential prefactors,  $De_0$ , and activation energies  $\Delta E$ . These results were analyzed according to the Meyer-Neldel rule (MNR).

The plot of the logarithm of the exponential prefactor versus the activation energy for all 222,784 pixels is given in Figure 2. The activation energies vary from roughly half the band-gap of Si to about the band-gap of Si, with most pixels having  $\Delta E$ 's of approximately 0.9 eV to 1 eV. The agreement of all data points with the MNR is remarkable. We can deduce the two MNR constants as  $E_{MN} = 25.3$  meV and  $De_{00} = 1685$  e/s. In order to get a better understanding of the meaning of these two constants, substituting Eq. (2) into Eq. (1) one obtains:

$$De = De_{00} \exp\left[\Delta E \left(\frac{1}{E_{MN}} - \frac{1}{kT}\right)\right] \quad (3)$$

Eq. (3) shows that for a characteristic temperature or energy the dark current is independent of the activation energy. This temperature, also known as isokinetic temperature, is given for our experiment as  $T_{MN} = E_{MN}/k = 294$  K.  $De_{00}$  is the dark current at the isokinetic temperature. The isokinetic temperature can also be seen in Fig. 1 as the intersection of the linear fits. At temperatures higher than the isokinetic temperature the MNR predicts an inversion of the dark current: pixels with dark current larger than the average at temperatures below  $T_{MN}$  have a dark current smaller than average above  $T_{MN}$ . In order to verify this prediction, the chip was heated to a temperature of 313 K. We found that the predicted inversion did not occur. It could only be found that the dark current was fairly similar for all pixels.

The linear relationship between the logarithm of the prefactor and the activation energy for all 222,784 pixels is remarkable, but the MNR does not predict the dark current close to and above the isokinetic temperature accurately. A closer look at the data set shows a positive curvature in the Arrhenius plot, and the apparent crossing in the Arrhenius plot is actually more a convergence of the dark currents for different pixels. As shown in Fig. 3, the average dark current is dominated by two activation energies. We have recently shown that a sum of two exponential processes with different activation energies can explain the observation of the MNR.[11]

### 3. SOURCES OF DARK CURRENT

Generally three different sources of dark current contribute to the total dark current in a CCD: the dark current generated in the depletion region, the diffusion dark current generated in the field-free region and the surface dark current. For a CCD operated in the MPP mode the surface generated dark current is almost completely suppressed. The analysis of the diffusion and depletion dark current is similar to the analysis of the dark current in a diode (see, for example, Grove[12] or Sze[13]).

#### 3.1. Depletion dark current

Assuming  $N_t$  traps present in the depletion region, located at energy  $E_t$  in the forbidden gap, and the cross-sections for holes and electrons are equal ( $\sigma_p = \sigma_n = \sigma$ ), the dark current in electrons per pixel per second is given by:

$$De_{dep} = \frac{n_i A_{pix} x_{dep}}{2\tau}, \quad (4)$$

where  $x_{dep}$  is the width of the depletion region,  $A_{pix}$  is the area of the pixel,  $n_i$  is the intrinsic carrier concentration, and the generation-recombination lifetime,  $\tau$ , is given by

$$\tau = \frac{\cosh\left(\frac{(E_i - E_t)/kT}{\sigma v_{th} N_t}\right)}{(\sigma v_{th} N_t)}, \quad (5)$$

where  $E_i$  and  $E_t$  are the intrinsic and trap energy levels, respectively, and  $v_{th}$  is the thermal velocity.

### 3.2. Diffusion dark current

The dark current diffusing from the neutral bulk in e/s is given as:

$$De_{diff} = \frac{D_n A_{pix} n_i^2}{x_{ff} N_A}, \quad (6)$$

where  $N_A$  is the acceptor concentration in the p-type substrate,  $x_{ff}$ , the width of the field free region between the depletion edge and the back surface of the die., and  $D_n$  is the diffusion coefficient for electrons. In deriving this expression, we have assumed that the excess electron concentration varies linearly with distance away from the depletion edge, i.e.,  $n = n_{po}x/x_{ff}$ .  $x_{ff}$  has replaced the diffusion length in the more conventional form of the equation.

The total dark current is given as the sum of the diffusion and the depletion dark currents as given by Eq. (4) and Eq. (6). Including the temperature dependence of  $n_i$ , this gives:

$$De = De_{o,diff} T^3 \exp\left(\frac{-E_g}{kT}\right) + De_{o,dep} T^{3/2} \exp\left(\frac{-E_g}{2kT}\right) \quad (7)$$

where  $E_g$  is the (temperature dependent) band gap of Si. Comparing with Eqs. (4) and (6) one obtains

$$De_{o,diff} = \frac{C^2 A_{pix} D_n}{N_A x_{ff}} \quad \text{and} \quad De_{o,dep} = \frac{C A_{pix} x_{dep}}{2\tau} \quad (8)$$

The diffusion dark current is proportional to  $n_i^2$  and the depletion dark current proportional to  $n_i$ .  $C$  is a constant involving the density of states in the conduction and valence bands ( $C = 3.28 \cdot 10^{-15} \text{ cm}^{-3} \text{ T}^{3/2}$ ). One can easily see that the first term increases in importance as the temperature increases. The second term will have a tendency to dominate at lower temperatures. It is commonly believed that the depletion dark current is dominant for temperatures close to or lower than room temperature. [14, 15] Hence, the activation energy for the dark current should be in the proximity of half the band-gap.

## 4. DATA ANALYSIS

In order to verify if the dark current in our CCD can be described by Eq. (7), we left both prefactors and activation energies as parameters and fit the data according to:

$$De = De_{o,diff} T^3 \exp\left(\frac{-\Delta E_{diff}}{kT}\right) + De_{o,dep} T^{3/2} \exp\left(\frac{-\Delta E_{dep}}{kT}\right) \quad (9)$$

These trials showed that indeed the assumptions leading to Eq. (9) were justified and accordingly, we fixed the activation energies to  $E_g$  and  $E_g/2$ , respectively. Using only the two prefactors as fitting parameters, we found, that, as expected,  $De_{o,diff}$  was very similar for all pixels ( $De_{o,diff} = \exp(34.9) \text{ e/K}^3$ ) and  $De_{o,dep}$  is characteristic for each pixel. As may be seen in Fig. 4 the data can be accurately modeled with Eq.(7).

From the fit of the data, it is possible to estimate the diffusion constant for the electrons and the trap density in the depletion regions. Inverting the equation for  $De_{o,diff}$  and solving for  $D_n$  yields,

$$D_n = \frac{N_A De_{o,diff} x_{ff}}{C^2 A_{pix}} \quad (10)$$

The CCD was built on  $\sim 30 \text{ } \Omega\text{-cm}$  material which gives  $N_A = 4 \cdot 10^{14} \text{ cm}^{-3}$ . With the depletion region  $\sim 3 \text{ } \mu\text{m}$  wide in MPP operation, the field free region on the  $14 \text{ } \mu\text{m}$  thick, thinned device is  $x_{ff} = \sim 11 \text{ } \mu\text{m}$ . This leads to a value of the diffusion constant of  $10.2 \text{ cm}^2/\text{s}$ . This is a reasonable value given the assumptions leading to the dark current expression.

We can calculate the electron lifetime in the depletion region from Eq. (8) as:

$$\tau = \frac{CA_{pix}x_{dep}}{2De_{o,dep}} \quad (11)$$

Although the values for  $De_{o,dep}$  varied for different pixels, its average value was measured as  $\exp(19) e/K^3$ . This leads to an average generation-recombination lifetime in the depletion region of 15.8 ms. Using this value for the g-r lifetime allows one to estimate the impurity concentration from Eq. (5)

$$N_t = \frac{\cosh\left(\frac{(E_i - E_t)/kT}{kT}\right)}{\sigma v_{th} \tau} \quad (12)$$

It is important to note that  $\tau$  will be temperature dependent if the impurity centers are not located at midgap. Our analysis shows that impurities, roughly at mid-gap, are responsible for the depletion current. Modeling our data required only the assumption of different concentrations of mid-gap impurities. This does not exclude the possibility that different impurities located close to mid-gap are responsible for the electron generation. Such impurities could for example be Ni, Co, Au which are close to the mid-gap and to a lesser extent Fe which is further away from the mid-gap.[16-19]. Assuming the mid gap impurity Au, which has a capture cross section  $\sigma_{Au} = \sim 1 \cdot 10^{-15} \text{ cm}^2$ , and  $v_{th} = 10^7 \text{ cm/s}$ , leads to a concentration of  $\sim 6.3 \cdot 10^9 \text{ cm}^{-3}$  or about 10 atoms /pixel.

## 5. CONCLUSION

In conclusion, we showed that analyzing dark current according to the Arrhenius law leads to a spread in the apparent activation energies with a mean value of approximately 1 eV. These activation energies and the corresponding prefactors were related as predicted by the MNR. The inversion in the dark current, predicted by the MNR, for temperatures higher than the isokinetic temperature was not observed. We found that with increasing temperature the dark current for different pixels was getting more uniform. This can be explained by a transition from the depletion dark current to diffusion dark current with increasing temperature. The diffusion dark current was dominant at temperatures lower than commonly assumed. All dark current measurements could be modeled by different concentrations of a single impurity complex. The identification of the impurities requires more detailed measurements of dark current using Dark Current Spectroscopy.[17-19] Also for future work, it would be of interest to understand how the diffusion dark current changes with different sizes of the field-free region.

## 6. REFERENCES

1. R. Widenhorn, L. Mündermann, A. Rest, and E. Bodegom, J. Appl. Phys **89**, 8179, (2001).
2. W. Meyer and H. Neldel, Z. Tech. Phys. **12**, 588, (1937).
3. D. G. Papageorgiou, G. A. Evangelakis, Surface Science **461**, L543, (2000).
4. X. L. Wu, R. Shinar, and J. Shinar, Phys. Rev. B **44**, 6161, (1991).
5. Y. Lubianiker and I. Balberg, Phys Rev. Lett. **78**, 2433, (1997).
6. K. Shimakawa and F. Abdel-Wahab, Appl. Phys. Lett. **70**, 652, (1996).
7. Y. F. Chen and S. F. Huang, Phys. Rev. B **44**, 13775, (1991).
8. H. Overhof and P. Thomas, "Electronic Transport in Hydrogenated Amorphous Semiconductors," (Springer-Verlag, Berlin, (1989).
9. A. Yelon, B. Movaghar and H.M. Branz, Phys. Rev. B **46**, 12244, (1992).
10. A. Yelon and B. Movaghar, Appl. Phys. Lett. **71**, 3549, (1997).
11. R. Widenhorn, A. Rest, E. Bodegom, "The Meyer-Neldel rule for a property determined by two transport mechanisms," to be published.
12. A. S. Grove, "Physics and Technology of Semiconductor Devices," (John Wiley & Sons, 1967).
13. S.M. Sze, "Physics of Semiconductor Devices," second edition (John Wiley & Sons, 1981).
14. M. J. Howes and D. V. Morgan, "Charge-Coupled Devices and Systems," (John Wiley & Sons, 1979) p. 17.
15. J. R. Janesick, "Scientific Charge-Coupled Devices," (SPIE Press, 2001).
16. R. D. McGrath, J. Doty, G. Lupino, G. Ricker, and J. Vallergera, IEEE Trans. Electron Devices, vol. ED-**34**, 2555, (1987).
17. W. C. McColgin, J. P. Lavine, J. Kyan, D. N. Nichols, and C. V. Stancampiano, International Electron Device Meeting 1992, p.113, (13-16 Dec., 1992).
18. W. C. McColgin, J. P. Lavine, and C. V. Stancampiano, Mat. Res. Soc. Symp. Proc. **378**, 713, (1995).
19. W. C. McColgin, J. P. Lavine, C. V. Stancampiano, and J. B. Russell, Mat. Res. Soc. Symp. Proc. **510**, 475, (1998).

7. FIGURES

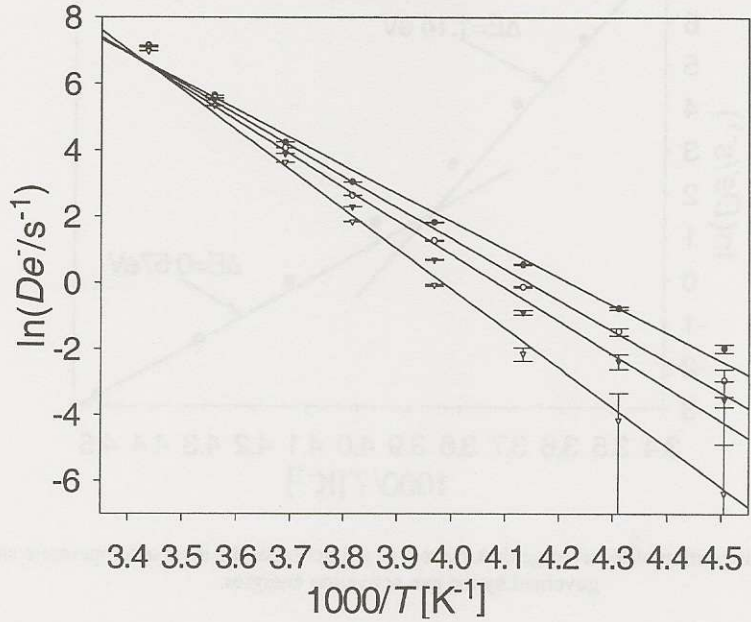


FIG. 1. The logarithm of the dark current as a function of the inverse temperature and linear fits for four different pixels.

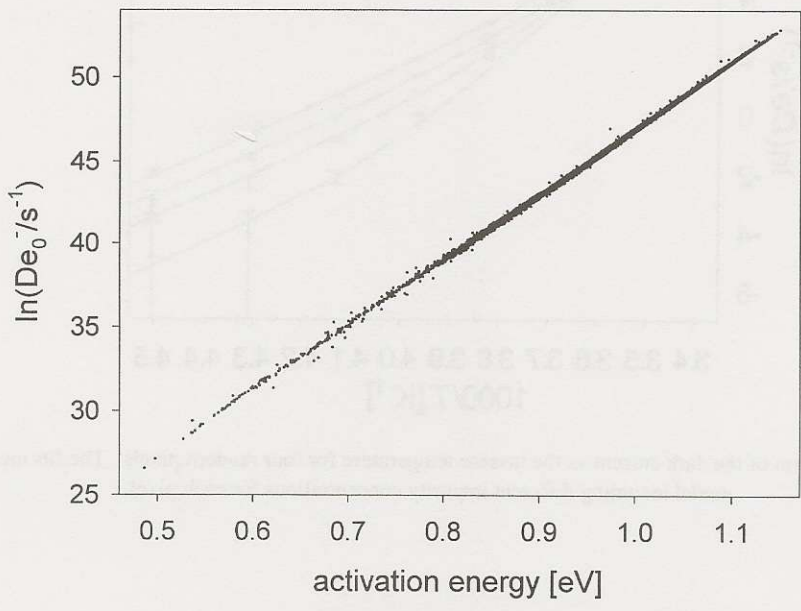


FIG. 2. The logarithm of the exponential prefactor as a function of the apparent activation energy for all pixels on the CCD-chip.

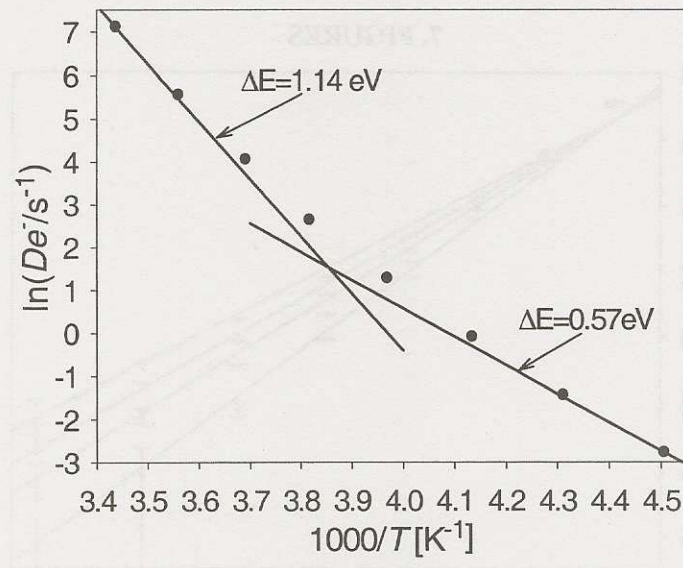


FIG. 3. Graph of the logarithm of the average dark current as a function of the inverse temperature showing regions governed by the two activation energies.

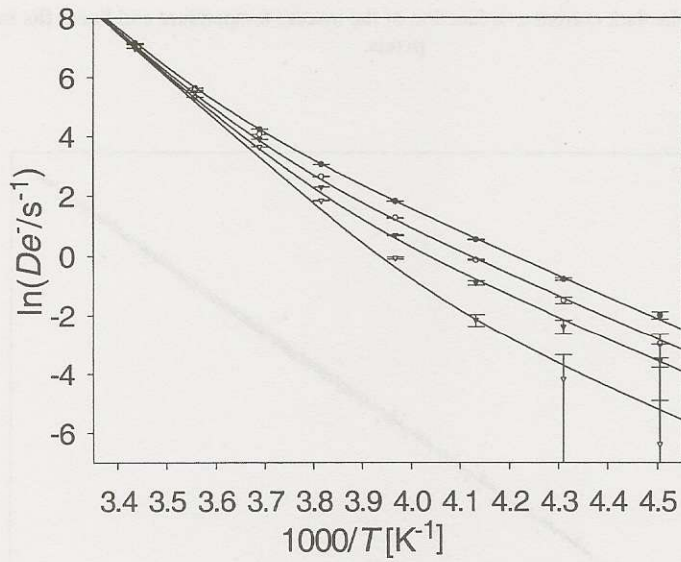


FIG. 4. The logarithm of the dark current vs the inverse temperature for four random pixels. The fits are based on the model assuming different impurity concentrations for each pixel.